SLAC–PUB–8966
August 2001

Monolithic I-Beam Crystal Monochromator

J. Bagnasco, D.G. Van Campen and T. Rabedeau

Stanford Synchrotron Radiation Laboratory, Stanford Linear Accelerator Center, Stanford University, Stanford, CA 94309

Abstract

Curved crystal, focusing monochromators featuring cubed-root thickness profiles typically employ side-clamped cooling to reduce thermally induced overall bend deformation of the crystal. While performance is improved, residual bend deformation is often an important limiting factor in the monochromator performance. A slightly asymmetric "I-beam" crystal cross section with cubed-root flange profiles has been developed to further reduce this effect. Physical motivation, finite-element modeling evaluation and performance characteristics of this design are discussed. Reduction of high mounting stress at the fixed end of the crystal required the soldering of an Invar support fixture to the crystal. Detailed descriptions of this process along with its performance characteristics are also presented.

Presented at Synchrotron Radiation Instrumentation Conference

Madison, Wisconsin, USA

August 22-24, 2001

Work supported in part by the Department of Energy contract DE-AC03-76SF00515.

1 Introduction

One of the important factors to improving synchrotron beam line performance is the reduction of the thermal deformation of the monochromator crystals. Manifestation of thermal deformation occurs through three separate but related effects: (i) Due to nonzero linear expansion, crystals experience lattice dilation proportional to the local crystal temperature. (ii) The applied power density produces a thermal bump and associated local rotation of crystal planes on the crystal surface. This effect is alleviated by aperturing a fraction of the total diffracted beam. (iii) Thermal gradients normal to the crystal surface produce a large-scale bend analogous to that of bimetallic strips. Minimization of this last effect is accomplished by positioning the heated surface near the neutral axis of the crystal where stress induced moments are equalized. This is the primary motivation for the I-beam crystal geometry discussed here.

2 Analysis of I-Beam Crystal

Curved crystal focusing monochromators are generally configured as cantilevered crystalline beams with the bend force applied to the free end of the crystal. To produce a constant radius of curvature the crystal stiffness is varied linearly along its length by either configuring the crystal with a triangular shaped diffracting surface of constant thickness or with a rectangular shaped diffracting surface of cubed root thickness profile. This later geometry is more compatible with side-clamped cooling but still suffers from some thermally induced overall bend distortion. Modifying this geometry to the asymmetric I-beam cross section depicted in Figure 1 minimizes the residual bend deformation of the

crystal. Here, the flange width h is varied to produce the cubed-root profile while the web is offset to minimize bend deformation.

The general equation to determine the deflection of a beam is[1]

$$EI(x)\frac{d^2y}{dx^2} = M(x) \tag{1}$$

where E is the Young's Modulus, $I(x)$ is the moment of inertia, and R is the radius of curvature with $1/R \approx \frac{d^2y}{dx^2}$. Function $M(x)$ is the applied moment at a point along the length of the crystal. For a cantilever supported crystal of length L, bent by an applied end force F, the moment of inertia is

$$I(x) = \frac{RF(L-x)}{E} \tag{2}$$

For an asymmetric I-beam crystal, $I(x)$ is

$$I(x) = \frac{2sh^3(x) + bt^3}{12} + (d - y_{cm}(x))^2 bt + 2(\frac{h(x)}{2} - y_{cm}(x))^2 sh(x) \tag{3}$$

where the parameters are defined in figure 1. The first term in equation 3 is for a symmetric I-beam. The remaining terms are contributions due to web offset. Center of mass, y_{cm} is determined using the formula

$$y_{cm}(x) = \frac{sh^2(x) + btd}{2sh(x) + bt} \tag{4}$$

Equations 3 and 4 are the exact. They allow $h(x)$ to be determined precisely for any arbitrary offset d. Unfortunately, when combined, they represent a fifth order polynomial that is difficult to solve using a finite element analysis (FEA) program. Fortunately, due to the smallness of the $(d - y_{cm}(x))^2$ term, it is convenient to treat it as a constant and solve for $h(x)$. Using equation 2, $h(x)$ is approximated by the expression

$$h(x) = [\frac{3RF}{2Es}(L-x) - \frac{bt^3}{8s} - \frac{3}{2s}(d - y_{cm})^2 bt - y_{cm}^3]^{\frac{1}{3}} + y_{cm} \tag{5}$$

The moment of inertia, y_{cm}, is calculated once using the initial values $x = 0$ and $h(0)$. It is *not* calculated continuously as a function of beam position. The result further approximates $h(x)$, but differs no more than 5% when compared to the exact solution for any position along the the crystal from 0 mm to 50 mm. Therefore, any local deviation from the ideal radius of curvature is small and will have no noticeable effect the performance of the crystal. Left unchecked, $h(x)$ will decrease to a width equivalent to the thickness of the web and eventually become negative before reaching the end of the crystal. This is due to the negative terms in equation 5. A composite beam was chosen to solve this problem. A sufficient region of the crystal implemented the cubed root geometry while the remainder used a rectangular cross section.

The crystal was modeled *in situ*, located between two glidcop cooling pads. A layer of $0.001''$ thick indium-gallium eutectic[2] was applied between each pad and the crystal, providing a conduction mediator and lubricant. The applied power was modeled as a rectangular cross section having an average power density of 13.16 W/mm^2. Power was applied over a length of 31 mm, starting 2 mm downstream from the supported end of the crystal.

For analysis $h(0)$ and displacement d were set to predetermined values where the *maximum* tensile stress was 5000 psi. Then, $h(0)$ was lowered by 0.01 mm increments until minimal crystal end deflection was located. For an end deflection δ, the average angular curvature was calculated using

$$\Delta\phi = \frac{2\delta}{L_{eff}} \tag{6}$$

where $L_{eff} = 50\ mm$ is the approximate effective cooling length of the crystal; no appreciable thermal bending occurs beyond it. For the asymmetric crystal, typical values for $\Delta\phi$ were $\sim 0.5\ \mu rad$ which is negligible relative to the Darwin width. Deflections were also evaluated at positions 1/4 and 3/4 down the length of the beam footprint. The difference between these locations was found to be $\sim 10^{-5}\ mm$, implying the slope along

the length of the crystal is small. Increasing the power density by 33%, while keeping the I-beam geometry constant, showed no appreciable change in these results.

For comparison, a symmetric crystal was analyzed. The web was positioned at the midpoint of the flanges. All other dimensions were *identical* to the asymmetric case. For each model displacement along the crystal center was recorded. These data are displayed in figure 2. Negative deflection of the symmetric case implies curvature away from power loaded side of crystal. Average angular curvature for the symmetric crystal is large, corresponding to $\Delta\phi \sim 180\ \mu rad$ which is several times the Darwin width. This result is better than rectangular cross section cubed-root crystals currently in use, but much poorer than the results of the asymmetric case.

3 Stress-Free Soldering of Invar to Silicon

Prior to construction of the beam line 11-1 monochromator, bent crystal designs at SSRL employed rigidly clamped supports coupled with a post style pivot contact. An applied force to the freestanding cantilever end was countered by these supports, producing a moment about the pivot post and generating a bending radius. These designs were practical, easy to assemble and compliant with ultra high vacuum (UHV) specifications. Unfortunately this concept was impractical for the beam line 11-1 project. Large, uneven loading produced local stress concentrations above the tensile limit of silicon; fracturing of test crystals was not uncommon. Typical fracture areas were about the post contact and flange edges in contact with the supports.

Soldering of support plates to the crystal was proposed[3] to alleviate these stress problems. Distribution of the bending force over a larger contact area and elimination of the post pivot would reduce stresses below the tensile limit, allowing the crystal to operate at the minimal required bending radius. In developing this concept, three issues were addressed[4]: (i) The soldering must withstand the stress associated with maximum

required end force applied to the crystal, preferably twice this limit. The solder should have sufficiently high Young's modulus to eliminate material fatigue. Specifically, deterioration caused by creep. (ii) The soldering process should produce minimal residual thermally induced stress between invar and silicon, reducing the possibility of a broaden rocking curve. (iii) For general applicability considerations, the soldering process must be UHV compatible.

Soldering is favorable to brazing due to the relatively low set-up temperature required for it. This reduces thermal stress contributions associated with differing linear expansion between dissimilar mating materials. After considering the operational temperature of the crystal and the relatively high temperatures due to bake-out procedures, a tin/antimony Sn(95%)/Sb(5%) alloy was selected as solder material. This alloy has good shear strength at 100^oC, is liquidus above 240^oC and solidus below 235^oC.

An invar alloy having composition 39% nickel was chosen as the support material. When compared to silicon, the difference in thermal expansion is $<$ 50 ppm between the temperature range $25^oC - 240^oC$. To insure good metal-to-metal contact and protection from surface oxidation the invar was prepared using the following procedure: (a) Material was cleaned and slightly etched to remove native oxide layer along with any contaminants. (b) Electroplate $1.3 - 2.0$ μm Ni using a UHV compatible nickel sulfamate process. (c) Electroplate 3000 Å Au. The gold layer serves as a protective coating against oxidation.

Surface preparation of the silicon crystal was more involved, but necessary to guarantee good adhesion to the silicon surface. The crystal was prepared using the following procedure: (a) Degrease and vacuum clean silicon crystal. (b) Etch surface with hydrofluoric acid (HF) to remove native oxide and remaining contaminants. (c) Coat surface with 150 Å Ti, 1275 Å Ni and 3000 Å Au, in this order, without breaking vacuum.

Prepared invar supports and the silicon crystal were assembled with a $0.002''$ Sn/Sb ribbon placed between them. The area of the solder joint was approximately $3/4''$ x $1/2''$ for each support. The assembly was placed inside a hydrogen braze furnace and heated to

250^oC, then allow to cool to room temperature.

Mechanical testing of the I-beam crystal was performed prior to full assembly. The crystal was bent to twice the minimal required bending radius, to a value of $R \approx 22\ M$ and remained in this configuration for approximately 12 hours. After this period no measurable displacement was detected, the solder joint showed no signs of fatigue or creep.

Diffraction rocking curves were taken at two positions on the crystal. At locations near and away from the solder joint, vertical scans over the central region of the crystal were performed. Within the uncertainty of the equipment, data showed no discernible difference between these locations. Thermal stress contributions due to soldering were not detected.

4 Conclusion

By adjusting the position of the web in the I-beam crystal we have shown it is possible to minimize the large-scale deformation of curved focusing monochromator crystals. Energy resolution of the crystal was substantially enhanced, improving the overall performance of the monochromator.

Attaching the silicon crystal to invar supports using a solder process provided an alternative approach to traditional mounting techniques. It reduced overall tensile stress in the crystal and proved resilient when subjected to excessive force, showing no signs of fatigue or failure. The solder solidifies at low temperature, is UHV compatible and produced no residual stress in the silicon crystal.

Acknowledgments

The authors would like to thank M. Rowen and G. Andronaco for fruitful discussions and technical assistance. We would also like to thank T. Gathright and W. Hollenbeck for technical assistance involving the solder process.

This work was conducted at the Stanford Synchrotron Radiation Laboratory, a national user facility operated by Stanford University on behalf of the U.S. Department of Energy, Office of Basic Energy Sciences under DOE contract DE-AC03-76SF00515

References

[1] S.P. Timoshenko, *Strength of Materials*, 3rd ed., Van Nostrand Reinhold, 1955.

[2] A.M. Khounsary *et al., SPIE,* **3151**, 45(1997).

[3] M. Rowen, private communication.

[4] D.G. Van Campen, *SSRL - BL11-1 - Low Stress Soldering Invar to Silicon*, SSRL internal pub. Eng. Note **M386** , September, 2000.

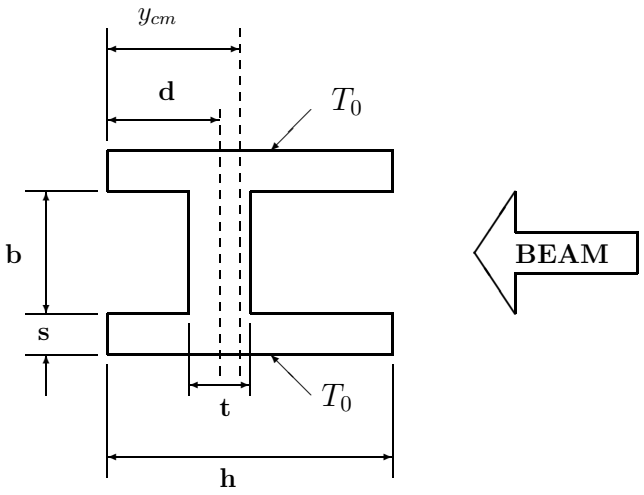
y_{cm}
d
T_0
b
BEAM
s
T_0
t
h

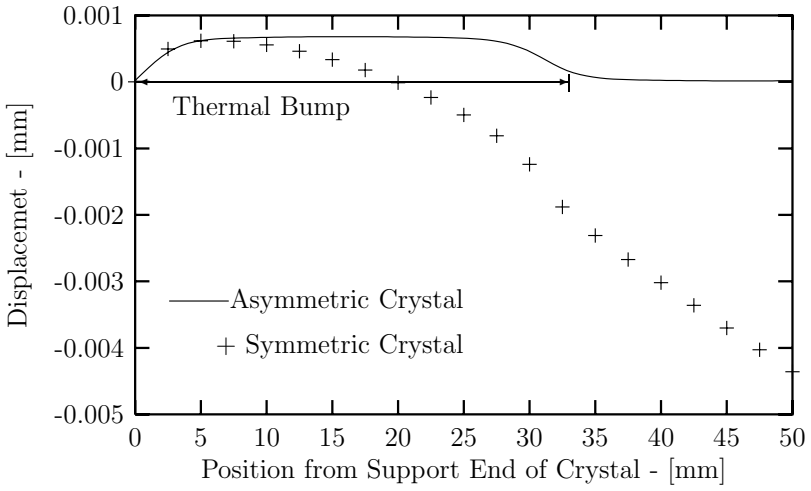
0.001
0
-0.001
-0.002
-0.003
-0.004
-0.005
Displacemet - [mm]
Thermal Bump
Asymmetric Crystal
+ Symmetric Crystal
0
5
10
15
20
25
30
35
40
45
50
Position from Support End of Crystal - [mm]

Figure 1: Asymmetric I-Beam Cross Section

Figure 2: Asymmetric vs Symmetric Crystals: Deflection Profiles